Eur. Phys. J. A **28**, 205–211 (2006)
DOI 10.1140/epja/i2006-10039-3

THE EUROPEAN PHYSICAL JOURNAL A

The effect of quark exchange in $\mathcal{A} = 3$ mirror nuclei and neutron/proton structure functions ratio

M. Modarres[1,a], M.M. Yazdanpanah[2], and F. Zolfagharpour[1]

[1] Physics Department, University of Tehran, 1439955961 Tehran, Iran
[2] Physics Department, Shahid-Ba-Honar University, Kerman, Iran

Received: 9 January 2006 / Revised: 14 March 2006 /
Published online: 12 June 2006 –
Communicated by V. Vento

Abstract. By using the quark-exchange formalism, the realistic Faddeev wave function and the Fermi motion effect, we investigate the deep inelastic electron scattering from $\mathcal{A} = 3$ mirror nuclei in the deep-valence region. The initial valence quark input is taken from the GRV's (Glück, Reya and Vogt) fitting procedure and the next–to–leading-order QCD evolution on $F_2^p(x, Q^2)$ which gives a very good fit to the available data in the (x, Q^2)-plane. It is shown that the free neutron to proton structure functions ratio can be extracted from the corresponding EMC ratios for ^{3}He and ^{3}H mirror nuclei by using the self-consistent iteration procedure and the results are in good agreement with the other theoretical models as well as the present available experimental data and especially the projected data expected from the proposed 11 GeV Jefferson Laboratory in the near future.

PACS. 13.60.Hb Total and inclusive cross sections (including deep-inelastic processes) – 21.45.+v Few-body systems – 14.20.Dh Protons and neutrons – 12.39.Ki Relativistic quark model

1 Introduction

In the framework of the *Standard Model*, the hadrons are composed of valence quark, sea quark and gluon [1]. In recent years, in order to test the perturbative and non-perturbative nature of quantum chromodynamics (QCD), most of the experiments and theoretical works have been focused on the studies of hadrons (mainly the proton and neutron) structure functions (SF) at the small-x (x is the Bjorken scaling variable) regions [2] where the sea quark and the gluon play an important role. While the middle-x region, *i.e.* $0.3 < x < 0.6$ at moderate Q^2 (the photon 4-momentum), has been assumed to be understood and can be explained by the valence quark dynamics, there is a lack of information about the nucleon structure function in the deep-valence region, $x > 0.6$, at any Q^2. There are a few reasons to study the quark distribution in nucleon at large x. The d/u quark distribution function ratio near $x \simeq 1$ can give information about 1) the spin-flavour symmetry breaking in the nucleon, 2) the onset of perturbative behavior [3] and 3) searching for the new physics beyond the *Standard Model* [4] in the high-energy colliders at high Q^2, *e.g.*, the uncertainty in the gluon distribution.

While the proton structure functions are quite well known both experimentally and theoretically [1–3], the neutron structure functions should usually be extracted from the deuterium and because of the large nuclear correction, there could be uncertainties as large as 50% in the d/u or $F_2^n/F_2^p \simeq \frac{1+4\frac{d}{u}}{4+\frac{d}{u}}$ ratios [5]. The bounds value of $\frac{1}{4} \leq \frac{F_2^n}{F_2^p} \leq 4$ has been proposed by Nachtmann [6] for the whole x regions. On the other hand, based on different models, the values of $\frac{2}{3}$ (the $SU(6)$ symmetry) [7], $\frac{1}{4}$ (the phenomenological and Regge considerations) [8] and $\frac{3}{7}$ (the quarks counting rules and perturbative QCD) [9] have been predicted as $x \longrightarrow 1$.

Recently, the possible use of an unpolarized tritium target has been proposed, by using the 11 GeV upgraded beam of the Jefferson Laboratory [10], and aimed at measuring F_2^n, using the ratio of structure functions of helium 3 ($\mathcal{F}_2^{^3He}$) to tritium ($\mathcal{F}_2^{^3H}$) in order to reduce the systematic errors both in the experimental measurements and theoretical calculations (which are model dependent).

The quark-exchange formalism (QEF) was originally introduced by Hoodbhoy and Jaffe (HJ) to investigate the quark distribution in the nuclear system [11,12]. Then, QEF was applied by one of the authors (MM) to light nuclei [13] and nuclear matter [14] and it was reformulated to derive the spin structure function of the three-nucleon system as well as the proton and neutron [15]. Finally, QEF was used as the initial condition for the QCD evolution

[a] e-mail: modarres@khayam.ut.ac.ir

equations [16] to calculate the sea quark and gluon contributions to the proton structure function at the leading- and the next–to–leading-order (NLO) levels. In most of the above calculations we found satisfactory agreement between our results and the available experimental data. So we claim that the quark-exchange formalism is a good motivation to investigate the behavior of the F_2^n/F_2^p ratio at the deep-valence region, *i.e.* $x \geq 0.6$.

Several groups have paid attention to the above issue [17–22] and they have used different models (mostly based on the impulse formalism and different spectral function approximation) to propose the F_2^n/F_2^p ratio at the deep-valence region. We will present their results in this work and compare them with ours. Recently, we also made a primary work in this direction by considering only the quark-exchange effect in the three-nucleon system. The result was encouraging (see, Modarres and Zolfagharpour [15]).

So, the paper will be organized as follows: In sect. 2, by using QEF, we present the valence quark momentum distribution for the proton and neutron in the ^{3}He and ^{3}H mirror nuclei (QEF is briefly explained in the appendix). Then, the structure functions of helium 3 and tritium are calculated by including both the quark exchange and the Fermi motion effects. The self-consistent calculation (the iteration procedure) of the ratio F_2^n/F_2^p will be explained in sect. 3. Finally, in sect. 4 we present our numerical results, discussion and conclusion.

2 Nucleus structure function

The structure function measures the quark distribution as a function of k^+ (the light-cone momentum of the initial quark) in the target rest frame which is equivalent to boosting the nucleus to an infinite momentum frame. This is usually done by using an *ad hoc* prescription for $k^0 = [(\vec{k}^2 + m^2)^{\frac{1}{2}} - \epsilon_0]$ as a function of $|\vec{k}|$ where m and ϵ are the *constituent quark mass* and *binding energy*, respectively. It has been shown that the resulting structure function is not sensitive to this assumption [11,23].

Because of the Gaussian choice of the quark wave function in QEF, we cannot consider the full GRV's SF, *i.e.* we should ignore the sea quark and gluon contributions to the SF. But this is a good approximation, since we are interested in the deep-valence region and the EMC ratios. So, the valence quark distribution at each Q^2 is related to the momentum distribution for each flavour in the nucleon of the nucleus $\mathcal{A}_i$ according to the following equation ($j = p, n$ ($a = u, d$) for proton (up-quark) and neutron (down-quark), respectively):

$$q_j{}^a(x, Q^2; \mathcal{A}_i) = \int \rho_a^j(\vec{k}; \mathcal{A}_i)\delta\left(x - \frac{k_+}{M_j}\right) \mathrm{d}\vec{k}. \quad (1)$$

By performing the angular integration, we get,

$$q_j{}^a(x, Q^2; \mathcal{A}_i) = 2\pi M_j \int_{k_{min}^{j,a}}^{\infty} \rho_a^j(\vec{k}; \mathcal{A}_i) k \mathrm{d}k \quad (2)$$

with

$$k_{min}^{j,a}(x) = \frac{(xM_j + \epsilon_0^{j,a})^2 - m_a^2}{2(xM_j + \epsilon_0^{j,a})}, \quad (3)$$

where $m_a(M_j)$ are the quarks (nucleons) *masses*, $\epsilon_0^{j,a}$ are the quark *binding energies* and $\rho_a^j(\vec{k}; \mathcal{A}_i)$ are the quark momentum distributions. Note that, regarding our Gaussian choice for the nucleon wave function in terms of quarks as illustrated in the appendix, near $x = 1$ the above prescription is not working properly because the structure function probes quark very far from their mass-shell [11,15]. For each Q^2 value, by using the fitting procedure which will be explained later on, it is possible to calculate the corresponding values of m_a and $\epsilon_0^{j,a}$. Then the target structure function $F_2^{\mathcal{A}_i}(x, Q^2)$ can be expressed in terms of the valence quark distribution as follows (Q_a are the quarks charges):

$$F_{2,ex}^{\mathcal{A}_i}(x, Q^2) = x \sum_{a=u,d;j=p,n} Q_a^2 q_j{}^a(x, Q^2; \mathcal{A}_i). \quad (4)$$

Similarly to our recent work [15], in order to fix the values of m_a and $\epsilon_0^{j,a}$ (for simplicity we drop the index j on $\epsilon_0^{j,a}$ and we assume $M = M_j = \frac{M_p + M_n}{2}$) we apply the above equations as well as the quark-exchange formalism to the proton ($\mathcal{A}_i = 1, \mathcal{M}_T = \frac{1}{2}$) as our target (obviously by considering the proton as our target there is no exchange term, *i.e.* $B = C = D = 0$ in eqs. (A.7)-(A.14), and we have just the direct term). In this case for each value of b we find the pairs m_a and ϵ_0^a [15] such that we get the best fit to the valence u and d quarks distribution functions of the GRV's proton structure function [24] (valence-SF). The GRV's proton structure function fits the experimental proton structure function data over the whole range of the (x, Q^2)-plane very well. Figure 1 (this figure is similar to the figure we have given in our recent work (Modarres and Zolfagharpour), ref. [15]) shows our fitted proton $F_{2,v}^p(x, Q^2)$ (neutron, $F_{2,v}^n(x, Q^2)$) structure function, obviously only for the valence quark, with $b = 0.8\,\mathrm{fm}$ (the charge radius of helium 3 and of tritium is produced with $b = 0.837$ and $0.78\,\mathrm{fm}$, respectively. So $b = 0.8\,\mathrm{fm}$ is a good choice) and the (m_a, ϵ_0^a) pairs of $(120\,\mathrm{MeV}, 150\,\mathrm{MeV})$ and $(140\,\mathrm{MeV}, 230\,\mathrm{MeV})$ at $Q^2 = 4\,\mathrm{GeV}^2$. The dotted (dash-double-dotted) curve is that of GRV with only valence quarks. The experimental data of SLAC [19] and NMC [25] as well as the full GRV's NLO structure functions for proton (dashed curve) and neutron (dash-dotted curve) are also given for comparison. This figure shows that for $x \geq 0.2$ we get a very good fit to SF of GRV as well as to the available data. With the same parameters we can calculate the corresponding ^{3}He and ^{3}H structure functions which are uncertain because of the lack of information about the neutron structure function. Obviously, in general our method fails for $x \to 0$ (because of the fitting procedure). It is also not good as $x \to 1$ especially for the nucleus target, because we have ignored the Fermi motion effect by using the leading-order expansion in the quark-exchange formalism [11–15]. In order to take into account the Fermi motion effect for tritium

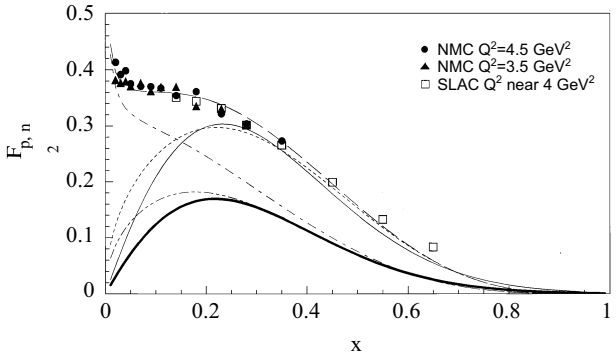

Fig. 1. The proton structure function, only with valence quark, for (m_a, ϵ_0^a) pairs of $(120\,\text{MeV}, 150\,\text{MeV})$ and $(140\,\text{MeV}, 230\,\text{MeV})$ at $Q^2 = 4\,\text{GeV}^2$ and $b = 0.8\,\text{fm}$ (full curve). The pairs $(120\,\text{MeV}, 150\,\text{MeV})$ and $(140\,\text{MeV}, 230\,\text{MeV})$ at $Q^2 = 4\,\text{GeV}^2$ have been chosen such that $b = 0.8\,\text{fm}$ gives the best fit to the GRV's valence quark distribution (dotted curve) [24]. The dashed and dash-dotted curves are the GRV's full NLO proton and neutron structure functions. The heavy full (dash-double-dotted) curve is the GRV's (our fitted) neutron structure function (at $b = 0.8\,\text{fm}$). The NMC and SLAC data [19,25] for the structure function of proton have been also given for comparison.

and helium 3, we can work in the convolution approach and in the harmonic-oscillator basis with the procedure described in refs. [1] and [26] as follows. In the convolution approach the nucleus structure function can be written as

$$F_2^{\mathcal{A}_i}(x, Q^2) = \sum_{j=p,n} \int_x^\infty \mathrm{d}z f_j{}^{\mathcal{A}_i}(z) F_2^j(x/z, Q^2), \qquad (5)$$

where $f_j{}^{\mathcal{A}_i}(z)$ and $F_2^j(x, Q^2)$ are the proton or neutron distribution functions in the target nucleus and the corresponding structure functions, respectively (where in this case, in order to calculate the Fermi motion effect without any approximation in the nucleon SF, we use the full GRV's structure functions, *i.e.* $F^p_{2,grv}(x, Q^2)$ and $F^n_{2,grv}(x, Q^2)$). In the harmonic-oscillator basis we have

$$f_j{}^{\mathcal{A}_i}(z) = \sum_{n_j, l_j} \mathcal{G}_{n_j,l_j} \mathcal{S}_{n_j,l_j}(z, M, \hbar\omega, \varepsilon_{n_j l_j}), \qquad (6)$$

where $\mathcal{G}_{n,l}$, $\mathcal{S}_{n,l}(z, M, \hbar\omega, \varepsilon_{nl})$, $\hbar\omega = \frac{\hbar^2\alpha^2}{M}$ and ε_{nl} are the occupation numbers, the sum of harmonic-oscillator polynomials (for the present calculation they are just a Gaussian function), the oscillator parameter and the single-particle energies [26]. For the three-body system $\alpha^2 = \frac{9}{2\langle r^2\rangle}$, where the rms radius $(\langle r^2\rangle)^{\frac{1}{2}}$ is 1.95 fm and 1.7 fm for helium 3 and tritium [27], respectively. We also set $\varepsilon_{nl} = 0$, since we only intend to calculate the Fermi motion contribution (the quark exchange is responsible for the binding effect). In fig. 2(a) the EMC ratios of ^{3}He to ^{3}H, *i.e.* $\mathcal{R}_{EMC}^{^3He,Fermi}(x, Q^2)/\mathcal{R}_{EMC}^{^3H,Fermi}(x, Q^2)$ by considering only the Fermi motion effect are plotted against x, where,

$$\mathcal{R}_{EMC}^{^3He,Fermi}(x, Q^2) = \frac{\mathcal{F}^{^3He}_{Fermi,2}(x, Q^2)}{2F^p_{2,grv}(x, Q^2) + F^n_{2,grv}(x, Q^2)},$$

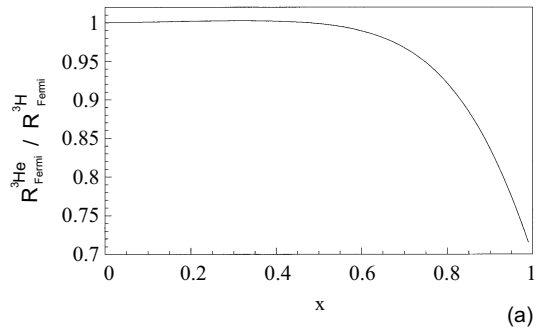

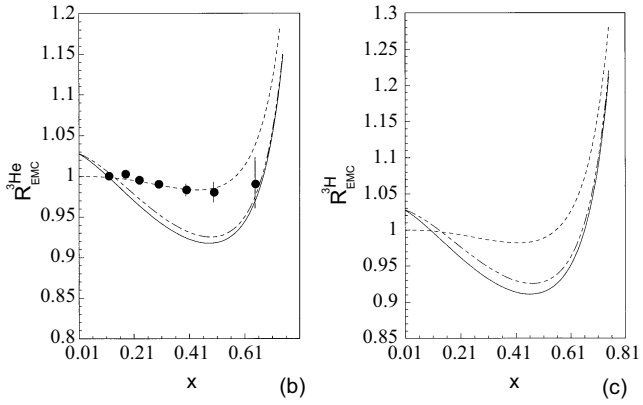

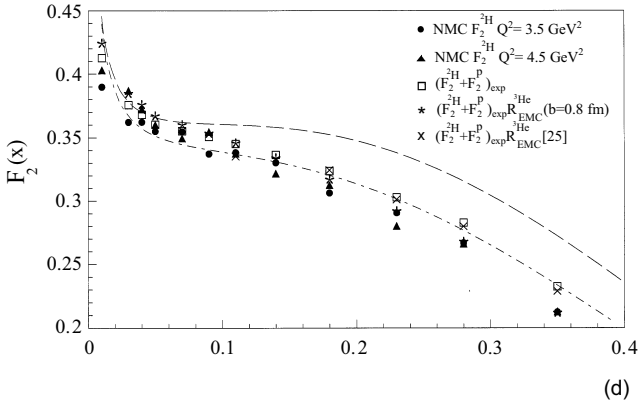

Fig. 2. (a) The EMC ratios of the structure functions of helium 3 to tritium by considering only the Fermi motion effect with the full GRV's proton and neutron structure functions. (b) The EMC effect in helium 3 and (c) in tritium for $b = 0.8\,\text{fm}$. The dotted curves are the corresponding Fermi motion effects. The data are from ref. [25]. The dash-dotted curves are after the second iterations. (d) The comparison of different structure functions. The dashed (dot-dashed) curve is that of GRV for proton, $F^p_{2,grv}(x, Q^2)$, $([2F^p_{2,grv}(x, Q^2) + F^n_{2,grv}(x, Q^2)]/3)$. See the text for details.

$$\mathcal{R}_{EMC}^{^3H,Fermi}(x, Q^2) = \frac{\mathcal{F}^{^3H}_{Fermi,2}(x, Q^2)}{F^p_{2,grv}(x, Q^2) + 2F^n_{2,grv}(x, Q^2)}. \qquad (7)$$

This figure shows that the Fermi motion is the same for helium 3 and tritium up to $x \simeq 0.6$ and since the size of ^{3}He is larger than ^{3}H, then for $x > 0.6$ the ratio starts to decrease, *i.e.* the Fermi motion effect has larger size in

tritium with respect to helium, as one should expect. An indistinguishable result is obtained if we use our fitted proton and neutron SF (valence-SF) instead of those of GRV (we explain the whole difference in fig. 5 and discuss this replacement).

Finally, the total structure functions for helium 3 and tritium can be written as the sum of the quark-exchange part, eq. (4) (obviously without the direct term, *i.e.* by considering $A = 0$ in eqs. (A.7)-(A.14), and the Fermi motion term, eq. (5):

$$\mathcal{F}_2^{\mathcal{A}_i}(x,Q^2) = F_{2,ex}^{\mathcal{A}_i}(x,Q^2)_{|_{A=0}} + F_{2,Fermi}^{\mathcal{A}_i}(x,Q^2). \quad (8)$$

We hope in our future works to omit this approximation by calculating the Fermi motion effect in the framework of QEF and the Faddeev wave function for the three-nucleon system (note that in this work, still the exchange term is calculated approximately because of the leading-order expansion of $\chi(\vec{p},\vec{q})$ we discussed earlier [15]).

3 Self-consistent treatment of F_2^n/F_2^p

By defining the EMC-type ratios for the structure functions of helium 3 and tritium (as the one we did for the Fermi motion effect) *i.e.*

$$\mathcal{R}_{EMC}^{^3He}(x,Q^2) = \frac{F_{2,ex}^{^3He}(x,Q^2)_{|_{A=0}}}{2F_{2,v}^p(x,Q^2) + F_{2,v}^n(x,Q^2)} + \frac{F_{2,Fermi}^{^3He}(x,Q^2)}{2F_{2,grv}^p(x,Q^2) + F_{2,grv}^n(x,Q^2)} \quad (9)$$

and

$$\mathcal{R}_{EMC}^{^3H}(x,Q^2) = \frac{F_{2,ex}^{^3H}(x,Q^2)_{|_{A=0}}}{F_{2,v}^p(x,Q^2) + 2F_{2,v}^n(x,Q^2)} + \frac{F_{2,Fermi}^{^3H}(x,Q^2)}{F_{2,grv}^p(x,Q^2) + 2F_{2,grv}^n(x,Q^2)}, \quad (10)$$

where we have used the appropriate neutron and proton structure functions for the quark exchange and Fermi motion parts of each nucleus structure function (*i.e.*, in order to calculate the numerator and denominator of the above ratios with the same approximation). We can also use the valence-SF in EMC ratios of the Fermi motions as well. Then we can calculate the above EMC ratios by using the fitted $(F_{2,v}^p(x,Q^2), F_{2,v}^n(x,Q^2))$ and the full GRV's $(F_{2,grv}^p(x,Q^2), F_{2,grv}^n(x,Q^2))$ proton and neutron structure functions (note that the fitted and the GRV's structure functions are very similar for $x > 0.25$), the convolution approach and the exchange part of quark-exchange formalism. In figs. 2(b) and (c) we have plotted these ratios for different values of b (fm). The dotted curves are the corresponding pure Fermi motion structure functions (obviously the differences between the full and dotted curves show the exchange parts of the quark-exchange model). So the quark exchange has sizable contribution up to $x \approx 0.63$ and it is larger for the helium 3 with respect to the tritium, as one should expect [15]. The HERMES helium 3 data are taken form ref. [25] at $Q^2 \simeq 7\,\mathrm{GeV}^2$. We should point out here that: i) The quoted data are the combinations of helium 3, deuterium and proton cross-sections (see Ackerstaff *et al.* [25] ($\mathcal{R} = \frac{\mathcal{F}_2^{^3He}}{\mathcal{F}_2^d + F_2^p}$)). ii) The structure function of helium 3 has been calculated by using various theoretical approximations and parameterizations which are valid for $x < 0.1$, especially the radiation corrections (see Ackerstaff *et al.* [25], p. 390, for details). So more experimental data is needed for a close comparison with the theoretical calculations. In order to clarify this point, in fig. 2d we have plotted the deuterium structure function data, the deuterium plus proton structure function data, our EMC result on helium 3 (the experimental EMC data) multiplied by the deuterium plus proton structure functions data. Now there is a very good agreement between our EMC result and the present available data, especially as we move to the larger x (there is no data for $x > 0.4$). In this region the EMC ratios are not very sensitive to the different values of b.

Now by dividing the above EMC ratios we can define the following equation:

$$\mathcal{R}_{EMC}^{^3He/^3H}(x,Q^2) = \frac{\mathcal{R}_{EMC}^{^3He}(x,Q^2)}{\mathcal{R}_{EMC}^{^3H}(x,Q^2)} = \mathcal{R}^{^3He/^3H}(x,Q^2) \times \left[\frac{1 + 2\mathcal{C}(x)F_{2,grv}^n(x,Q^2)/F_{2,grv}^p(x,Q^2)}{2 + \mathcal{C}(x)F_{2,grv}^n(x,Q^2)/F_{2,grv}^p(x,Q^2)}\right] \quad (11)$$

with

$$\mathcal{R}^{^3He/^3H}(x,Q^2) = \frac{\mathcal{F}_2^{^3He}(x,Q^2)}{\mathcal{F}_2^{^3H}(x,Q^2)}, \quad (12)$$

where we have introduced the unknown correction function $\mathcal{C}(x)$ to the GRV's neutron structure function $F_{2,grv}^n(x,Q^2)$. If the proton and neutron structure functions in $\mathcal{A} = 3$ nuclei were not dramatically different then one should expect that $\mathcal{R}_{EMC}^{^3He/^3H}(x,Q^2) \simeq 1$.

Equation (13) can be solved for the neutron to proton structure functions ratio, $\mathcal{C}(x) = F_{new,2}^n(x,Q^2)/F_{2,grv}^p(x,Q^2)$, in terms of the EMC ratio, $\mathcal{R}_{EMC}^{^3He/^3H}(x,Q^2)$, which directly yields

$$\mathcal{C}(x) = \frac{F_{new,2}^n(x,Q^2)}{F_{2,grv}^p(x,Q^2)} = \frac{2\mathcal{R}_{EMC}^{^3He/^3H}(x,Q^2) - \mathcal{R}^{^3He/^3H}(x,Q^2)}{2\mathcal{R}^{^3He/^3H}(x,Q^2) - \mathcal{R}_{EMC}^{^3He/^3H}(x,Q^2)}. \quad (13)$$

Equations (4)-(10) are coupled to eq. (13) in terms of the "new neutron structure function". So, for iteration, we consider the following structure functions as our input and we start from eq. (4):

$$\begin{aligned} &F_{2,grv}^p(x,Q^2) \to F_{2,grv}^p(x,Q^2),\\ &F_{2,grv}^n(x,Q^2) \to \mathcal{C}(x)F_{2,grv}^n(x,Q^2),\\ &F_{2,v}^p(x,Q^2) \to F_{2,v}^p(x,Q^2),\\ &F_{2,v}^n(x,Q^2) \to \mathcal{C}(x)F_{2,v}^n(x,Q^2). \end{aligned} \quad (14)$$

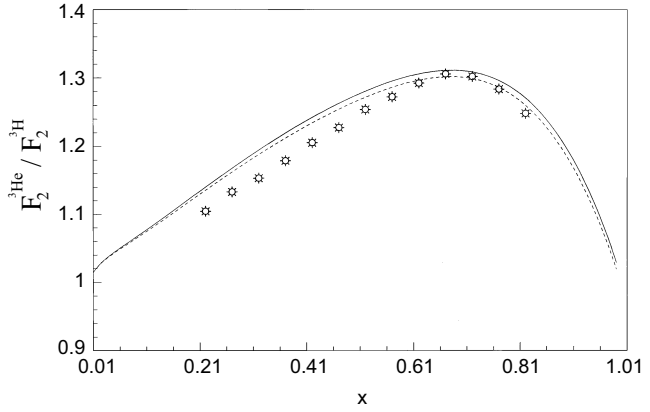

Fig. 3. (a) The ratios of structure functions of helium 3 to tritium (eq. (12)) for $b = 0.8$ fm (full curves). The dashed curve is after second iteration with $b = 0.8$ fm. The sun-burst points are from refs. [10,20] (see the text for details).

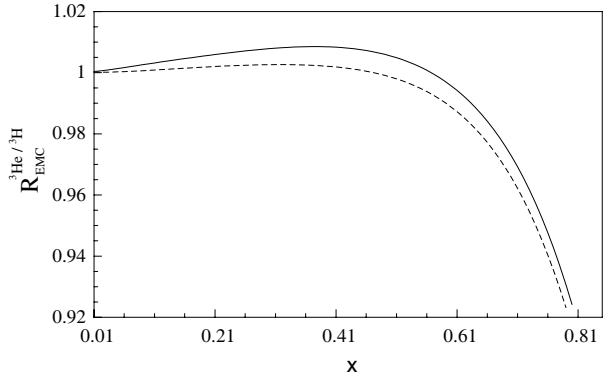

Fig. 4. The EMC ratios for $b = 0.8$ fm. The dashed curve is after second iteration with $b = 0.8$ fm.

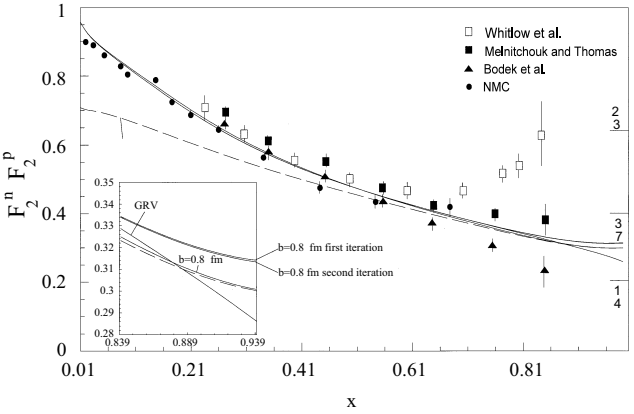

Fig. 5. The neutron to proton structure functions ratios (eq. (13), see the text for more details). The data are from Whitlow *et al.* [19], Melnitchouk and Thomas [18], Bodek *et al.* [17] and NMC [25]. The dashed curve is with the valence-SF in the EMC ratios of the Fermi motion effect.

(if we use the valence-SF in the EMC ratios of the Fermi motion effect, then obviously we only make the third and the fourth input replacements). With the above structure functions we again calculate the quark-exchange and Fermi motion effects, EMC ratio etc., in order to find another correction function $\mathcal{C}(x)$ and we continue this procedure until the iteration converges.

4 Result, discussion and conclusion

In fig. 3 the ratios of the structure functions of helium 3 to tritium (eq. (12)) are plotted for $b = 0.8$ fm (full curves). The dashed curve is the same ratio with $b = 0.8$ fm after the second iteration. The sun-burst points are the expected ratios that have been estimated by using the kinematics of the proposed 11 GeV Jefferson Laboratory experiment [10,20]. There is remarkable agreement between the estimated prediction [10,20] and the present calculation. The ratios remain the same if we use the valence-SF instead of GRV's SF in the Fermi motion effect.

The EMC ratios (eq. (11)) are plotted in fig. 4. In general, since 1) we have taken into account all of the properties of the structure functions of proton, neutron, helium 3 and tritium and 2) the proton and neutron structure functions are not dramatically too different (as is seen from fig. 1), it is expected that $\mathcal{R}_{EMC}^{^3He/^3H}(x, Q^2) \simeq 1$. However, this figure shows that the calculated EMC ratios have a very small variation from $\mathcal{R}_{EMC}^{^3He/^3H}(x, Q^2) = 1$ and this deviation increases as $x \to 1$ (which is mostly due to Fermi motion effect). A similar behavior is also seen in other calculations in which the impulse approximation has been used [20]. Again the dashed curve is the result of second iteration for $b = 0.8$ fm.

Finally, in fig. 5 the calculated neutron to proton structure functions ratios have been plotted for $b = 0.8$ fm. The large scale of this graph is also given for the deep-valence region. The third iteration is not distinguishable from the second one. The limiting values of above ratio for $x = 1$ (as it was discussed in the introduction) from different models are shown in the left side of this figure by arrows. The data are from refs. [17–19,25]. The iteration approximately converges after the third one. Our results are very closed to the present available data in the whole x region. The dashed curve is the neutron to proton structure functions ratio by using the valence-SF in the EMC ratios of the Fermi motion effect. As one should expect there is a small difference in the small-x region with respect to the full curve and it shows that the valence quarks are mainly responsible for the large-x region ($x > 0.3$). We observed that the variation of b, *i.e.* the nucleon size, only affects our results in the deep-valence region. Our calculated neutron to proton structure functions ratios are also in good agreement with the present theoretical calculation in which different models and approximations have been used [17–22].

In conclusion, we have calculated the helium 3 and tritium structure functions ratios in the framework of the quark-exchange model. We have treated u and d quarks as well as proton and neutron explicitly in our formalism and we have found satisfactory results compared to the present available data and others' theoretical models. In general, it is not correct to calculate the Fermi motion

and quark-exchange effect with different nucleon structure functions, as we did in present work. But, since we could not calculate the quark-exchange effect with the full GRV's structure functions, we used only the valence-SF of GRV in quark-exchange formalism as input. So, as we pointed out in the text before, we also divided the quark-exchange effect to the valence-SF to get the corresponding contribution of the EMC effect. Because, we should use the same approximation in the numerator and denominator of EMC ratio (in general, the numerator and denominator of a ratio has to be calculated with the same approximation, otherwise the ratio will be under- or overestimated).

Our results show that the quark-exchange effect is much larger in the three-nucleon system than previously thought [20]. We found that the EMC ratios of helium 3 and tritium are very similar for $x < 0.7$. Now, if this phenomenon also happens for heavier nuclei one can conclude that in general the "through" EMC ratios of the nuclei, *i.e.* $\mathcal{F}^{\mathcal{A}_i}(x,Q^2)/(Z_iF_2^p(x,Q^2)+N_iF_2^n(x,Q^2))$ would be roughly the same for all nuclei. This can also be explained by the saturation properties of nuclear forces [28]. However, we should point out that the three-body systems lie far from the saturation region of nuclear forces and we hope we could investigate this matter in our future works.

We can improve our calculation by i) treating the Fermi motion effect explicitly in the quark-exchange framework, *i.e.* calculating the leading-order expansion we made in the appendix [11–15] as well as using other choice of nuclear wave functions which have been calculated with the new nucleon-nucleon potentials [29], ii) evaluating the connected three-body diagram which has been ignored in the present calculation [15] and finally, iii) since for the nuclei one could have the non-vanishing structure function for x larger than one [30,31], we can measure and calculate this behaviour by considering the quark-exchange effect in nuclei with a full realistic nuclear wave function.

MM would like to thank the University of Tehran for supporting him under the grants provided by its Research Council.

Appendix A. Quark-exchange formalism

Let us start with a brief summary of the quark-exchange formalism. We take the nucleon states to be composed of three valence quarks [11,15],

$$|\alpha\rangle = \mathcal{N}^{\alpha^\dagger}|0\rangle = \frac{1}{\sqrt{3!}}\mathcal{N}^{\alpha}_{\mu_1\mu_2\mu_3}q^\dagger_{\mu_1}q^\dagger_{\mu_2}q^\dagger_{\mu_3}|0\rangle, \tag{A.1}$$

where α designate the nucleon states $\{\vec{P}, M_S, M_T\}$ and μ stand for the quark states $\{\vec{k}, m_s, m_t, c\}$, with the convention that there is a summation on the repeated indices as well as integration over $\vec{k}$. $q^\dagger$ ($\mathcal{N}^{\alpha^\dagger}$) are the creation operators for quark (nucleon) and $\mathcal{N}^{\alpha}_{\mu_1\mu_2\mu_3}$ are the totally antisymmetric nucleon wave functions, *i.e.*

$$\mathcal{N}^{\alpha}_{\mu_1\mu_2\mu_3} = D(\mu_1,\mu_2,\mu_3;\alpha_i) \times\delta(\vec{k}_1+\vec{k}_2+\vec{k}_3-\vec{P})\phi(\vec{k}_1,\vec{k}_2,\vec{k}_3,\vec{P}). \tag{A.2}$$

The $D(\mu_1,\mu_2,\mu_3;\alpha_i)$ depend on the Clebsch-Gordon coefficients $C^{j_1j_2j}_{m_1m_2m}$ and on the color factor $\epsilon_{c_1c_2c_3}$,

$$D(\mu_1,\mu_2,\mu_3;\alpha_i) = \frac{1}{\sqrt{3!}}\epsilon_{c_1c_2c_3}\frac{1}{\sqrt{2}}\sum_{s,t=0,1} C^{\frac{1}{2}s\frac{1}{2}}_{m_{s_\sigma}m_sM_{S_{\alpha_i}}} \times C^{\frac{1}{2}\frac{1}{2}s}_{m_{s_\mu}m_{s_\nu}m_s}C^{\frac{1}{2}t\frac{1}{2}}_{m_{t_\sigma}m_tM_{T_{\alpha_i}}}C^{\frac{1}{2}\frac{1}{2}t}_{m_{t_\mu}m_{t_\nu}m_t}. \tag{A.3}$$

The $\phi(\vec{k}_1,\vec{k}_2,\vec{k}_3,\vec{P})$ are the nucleon wave functions in terms of quarks and we write them in a Gaussian form ($b \simeq$ nucleons radius):

$$\phi(\vec{k}_1,\vec{k}_2,\vec{k}_3,\vec{P}) = \left(\frac{3b^4}{\pi^2}\right)^{\frac{3}{4}} \times\exp\left[-b^2\left(\frac{(k_1^2+k_2^2+k_3^2)}{2}+\frac{b^2P^2}{6}\right)\right]. \tag{A.4}$$

We can define the nucleus state based on the nucleon creation operators, *i.e.*

$$|\mathcal{A}_i=3\rangle = (3!)^{-\frac{1}{2}}\chi^{\alpha_1\alpha_2\alpha_3}\mathcal{N}^{\alpha_1{}^\dagger}\mathcal{N}^{\alpha_2{}^\dagger}\mathcal{N}^{\alpha_3{}^\dagger}|0\rangle, \tag{A.5}$$

where $\chi^{\alpha_1\alpha_2\alpha_3}$ are the complete antisymmetric nuclear wave functions which should be interpreted as the center-of-mass motion of the three-nucleon system. They are taken from the Faddeev calculation with the Reid soft core potential [15,32]. According to Afnan *et al.* [20], the choice of the nucleon-nucleon potential does not affect the EMC results. However, we will investigate this matter in our future works.

The quark momentum distribution with fixed flavour in a three-nucleon system is defined as,

$$\rho_{\bar{\mu}}(\vec{k};\mathcal{A}_i) = \frac{\langle\mathcal{A}_i=3|q^\dagger_{\bar{\mu}}q_{\bar{\mu}}|\mathcal{A}_i=3\rangle}{\langle\mathcal{A}_i=3|\mathcal{A}_i=3\rangle}, \tag{A.6}$$

where the sign bar means no summation on m_t and integration over $\vec{k}$ in the μ indices. By using the above definition, we can calculate the quark momentum distribution for each flavour. In the above equation we use, $\chi(x,y,\cos\theta)$, the Fourier transform of the nucleus wave function (as we said before it is taken from the solution of the Faddeev equation with the Reid soft core interaction). We only consider the leading-order expansion in $\chi(\vec{x},\vec{y})$ [11–15].

Finally, we get the resulting quark momentum distribution as follows [15]:

$$\rho^{^3He}(k) = \left[2A(k)+\frac{2}{9}B(k)+\frac{4}{9}D(k)\right]\left[1+\frac{9}{8}\mathcal{I}\right]^{-1}, \tag{A.7}$$

$$\rho^{^3H}(k) = \left[A(k)+\frac{1}{9}B(k)+\frac{4}{9}C(k)-\frac{2}{9}D(k)\right]\left[1+\frac{9}{8}\mathcal{I}\right]^{-1}, \tag{A.8}$$

where ($\mathcal{I}$ is the contribution of the nucleus wave function to the quark-exchange momentum distribution [11])

$$A(k) = \left[\frac{3b^2}{2\pi}\right]^{\frac{3}{2}}\exp\left[-\frac{3}{2}b^2k^2\right],$$

$$B(k) = \left[\frac{27b^2}{8\pi}\right]^{\frac{3}{2}} \exp\left[-\frac{3}{2}b^2k^2\right]\mathcal{I}, \tag{A.9}$$

$$C(k) = \left[\frac{27b^2}{7\pi}\right]^{\frac{3}{2}} \exp\left[-\frac{12}{7}b^2k^2\right]\mathcal{I},$$

$$D(k) = \left[\frac{27b^2}{4\pi}\right]^{\frac{3}{2}} \exp\left[-3b^2k^2\right]\mathcal{I}, \tag{A.10}$$

and obviously we have

$$\int \rho^{^3H}(k)\mathrm{d}\vec{k} = \frac{1}{2}\int \rho^{^3He}(k)\mathrm{d}\vec{k} = 1. \tag{A.11}$$

Similarly, we can find the up- and down-quark distributions (we assume $SU(6)$ symmetry):

$$\rho^u(k) = \left[2A(k) + \frac{2}{9}B(k) - \frac{16}{27}C(k) + \frac{28}{27}D(k)\right]\left[1 + \frac{9}{8}\mathcal{I}\right]^{-1}, \tag{A.12}$$

$$\rho^d(k) = \left[A(k) + \frac{1}{9}B(k) - \frac{20}{27}C(k) + \frac{26}{27}D(k)\right]\left[1 + \frac{9}{8}\mathcal{I}\right]^{-1}, \tag{A.13}$$

where

$$\int \rho^d(k)\mathrm{d}\vec{k} = \frac{1}{2}\int \rho^u(k)\mathrm{d}\vec{k} = 1. \tag{A.14}$$

See Modarres and Zolfagharpour [15] for details.

References

1. M.M. Sargsian *et al.*, J. Phys. G **29**, R1 (2003); G. Piller, W. Wesie, Phys. Rep. **330**, 1 (2000); L.L. Frankfurt, M.I. Strikman, Phys. Rep. **76**, 215 (1981).
2. B. Lampe, E. Reya, Phys. Rep. **332**, 1 (2000).
3. R.P. Feynman, *Photon Hadron Interactions* (Benjamin, New York, 1972); F.E. Close, *An Introduction to Quarks and Partons* (Academic Press, London, 1989); R.G. Roberts, *The Structure of the Proton* (Cambridge University Press, New York, 1993).
4. E. Eichten, I. Hinchliffe, K. Lane, C. Quigg, Rev. Mod. Phys. **56**, 579 (1984); S. Kuhlmann *et al.*, Phys. Lett. B **476**, 291 (2000); Daniel Stump *et al.*, JHEP **0310**, 046 (2003).
5. G.B. West, Phys. Lett. B **37**, 509 (1971).
6. O. Nachtmann, Nucl. Phys. B **38**, 397 (1972).
7. J. Kuti, V.F. Weisskopf, Phys. Rev. D **4**, 3418 (1971).
8. F.E. Close, Phys. Lett. B **43**, 422 (1973); R. Carlitz, Phys. Lett. B **58**, 345 (1975); F.E. Close, A.W. Thomas, Phys. Lett. B **212**, 227 (1988).
9. S.J. Brodsky, M. Burkardt, I. Schmidt, Nucl. Phys. B **441**, 197 (1995); G.R. Farrar, D.R. Jackson, Phys. Rev. Lett. **35**, 1416 (1975).
10. I.R. Afnan *et al.*, Phys. Lett. B **493**, 36 (2000); G.G. Petratos *et al.*, in *Proceedings of the International Workshop on the Nucleon Structure in the High x-Bjorken Region (HiX2000), Temple University, Philadelphia (PA), USA, March 30-April 1, 2000* (2000); W. Melnitchouk, in *Proceedings of the Workshop on the Experiments with Tritium at JLAB, Sept. 20-21, 1999, TJNAF, Newport (VA)*; G.G. Petratos *et al.*, in *Proceedings of the Workshop on the Experiments with Tritium at JLAB, Sept. 20-21, 1999, TJNAF, Newport (VA)*.
11. P. Hoodbhoy, R.L. Jaffe, Phys. Rev. D **35**, 113 (1987).
12. P. Hoodbhoy, Nucl. Phys. A **465**, 637 (1987).
13. M. Modarres, J. Phys. G **20**, 1423 (1994).
14. M. Modarres, K. Ghafoori-Tabrizi, J. Phys. G **14**, 1479 (1988).
15. M.M. Yazdanpanah, M. Modarres, Phys. Rev. C **57**, 525 (1998); M. Modarres, F. Zolfagharpour, Nucl. Phys. A **765**, 112 (2006).
16. M.M. Yazdanpanah, M. Modarres, Eur. Phys. J. A **6**, 91 (1999); **7**, 573 (2000); Few-Body Syst. **37**, 33 (2005).
17. A. Bodek *et al.*, Phys. Rev. D **20**, 1471 (1979).
18. W. Melnitchouk, A.W. Thomas, Phys. Lett. B **377**, 11 (1996).
19. L.W. Whitlow *et al.*, Phys. Lett. B **282**, 475 (1992).
20. I.R. Afnan *et al.*, Phys. Lett. B **493**, 36 (2000); I.R. Afnan *et al.*, Phys. Rev. C **68**, 035201 (2003); F. Bissey, A.W. Thomas, I.R. Afnan, Phys. Rev. C **64**, 024004 (2001).
21. C.J. Benesh, T. Goldman, G.J. Stephenson jr., Phys. Rev. C **68**, 045208 (2003); A.S. Rinat, M.F. Taragin, Phys. Lett. B **551**, 284 (2003).
22. E. Pace, G. Salme, S. Scopetta, A. Kievsky, Phys. Rev. C **64**, 055203 (2001); Nucl. Phys. A **689**, 453 (2001).
23. A. De Rujula, F. Martin, Phys. Rev. D **22**, 1787 (1980).
24. M. Glück, E. Reya, A. Vogt, Z. Phys. C **67**, 433 (1995); Eur. Phys. J. C **5**, 361 (1998).
25. M. Arneodo *et al.*, Nucl. Phys. B **483**, 3 (1997); K. Ackerstaff *et al.*, Phys. Lett. B **475**, 386 (2000).
26. S.V. Akulinichev, S. Shlomo, S.A. Kulagin, G.M. Vagradov, Phys. Rev. Lett. **55**, 2239 (1985).
27. R.C. Barrett, D.F. Jackson, *Nuclear Sizes and Structure* (Clarendon Press, Oxford, 1977).
28. M. Modarres, N. Rasekhinejad, Phys. Rev. C **72**, 014301 (2005).
29. M. Modarres, M.M. Yazdanpanah, F. Zolfagharpour, submitted to Phys. Rev. C (2005).
30. S.V. Akulinichev, S. Shlomo, Phys. Rev. C **33**, 1551 (1986).
31. I.A. Savin, *International Seminar on High Energy Physics, Dubna*, Joint Institute for Nuclear Research, Report No. D1, 2-81-728 (1981).
32. C.R. Chen, G.L. Payne, J.L. Friar, B.F. Gibson, Phys. Rev. C **33**, 1740 (1986); J.L. Friar, B.F. Gibson, E.L. Tomusiak, G.L. Payne, Phys. Rev. C **24**, 665 (1981); A. Stadler, W. Glöckle, P.U. Sauer, Phys. Rev. C **44**, 2319 (1991).